

Patterned and Controlled Polyelectrolyte Fractal Growth and Aggregations

Ilsoon Lee,* Jin Soo Ahn, and Troy R. Hendricks

Department of Chemical Engineering and Materials Science, Michigan State University,
East Lansing, Michigan 48824

Michael F. Rubner† and Paula T. Hammond‡

Departments of Chemical Engineering and Materials Science and Engineering,
Massachusetts Institute of Technology, Cambridge, Massachusetts 02139

Received September 26, 2003. In Final Form: December 12, 2003

Two-dimensional patterned and controlled polyelectrolyte aggregations (e.g., tree-like ramified structures) created by microcontact printing have been demonstrated and discussed. Polyelectrolyte-micropatterned aggregations on surfaces were controlled by the micropattern size and shape of PDMS stamps. The formation of aggregates was dependent on the ink and surface conditions, and the aggregates consisted of two distinct layers; strongly adsorbed, primary uniform layers and weakly adsorbed, secondary aggregation layers positioned on top of the primary layers. The adsorption of the primary layers was strong enough not to be washed away, while the aggregated secondary layers were easily removed by washing. The aggregation of secondary layers showed typical tree-like ramified structures of fractal growth and aggregation. Directional and confined stamping led to directing and confining the growth of the fractal polyelectrolyte clusters, respectively. The micropatterned primary uniform layers were not removed by extensive washing, and they were identified by selective nickel plating and charged particle selective adsorption in which the surface formed positive and negative micropatterns. These functional and patterned surfaces have great potentials for advanced devices and sensors.

Introduction

Thin film morphology on solid surfaces has attracted a great deal of attention for important industrial applications, such as coatings,^{1–4} adhesives,^{5–14} and optoelectronic display materials.^{15–17} Functional and topographic, regular or irregular patterned surfaces have gained a lot of interest,^{18–26} for practical purposes. Nonuniform struc-

tures such as ramified structures are generally caused by nonequilibrium phenomena due to interfacial instabilities. Such irregular patterns of ramified structures on surfaces are also considered as a broad class of patterning processes. Colloidal aggregation^{12,27–31}, dielectric breakdown,³² fractal hole growth in strained block copolymer films,³³ dendritic crystal growth,^{34–36} electrodeposition,³⁷ and viscous fingering in fluid flow,³⁸ related with fractal growth and aggregation phenomena, are of great interest in current research; these systems are the result of the micro- and

* Corresponding author. Fax: 517-432-1105. E-mail: leeil@egr.msu.edu.

† Department of Materials Science and Engineering.

‡ Department of Chemical Engineering.

- (1) Decher, G. *ACS Symp. Ser.* **1997**, *672*, 445–459.
- (2) Hattori, H. *Adv. Mater.* **2001**, *13*, 51.
- (3) Koetse, M.; Laschewsky, A.; Mayer, B.; Rolland, O.; Wischerhoff, E. *Macromolecules* **1998**, *31*, 9316–9327.
- (4) Muller, M.; Rieser, T.; Lunkwitz, K.; Meier-Haack, J. *Macromol. Rapid Commun.* **1999**, *20*, 607–611.
- (5) Bates, F. S.; Fredrickson, G. H. *Annu. Rev. Phys. Chem.* **1990**, *41*, 525–557.
- (6) Caseri, W. *Macromol. Rapid Commun.* **2000**, *21*, 705–722.
- (7) Imai, K.; Sato, T.; Senoo, H. *Cell Struct. Funct.* **2000**, *25*, 329–336.
- (8) Mercey, B.; Wolfman, J.; Raveau, B. *Curr. Opin. Solid State Mater. Sci.* **1999**, *4*, 24–27.
- (9) Prane, J. W. *J. Coat. Technol.* **1984**, *56*, 100–100.
- (10) Tsukruk, V. V. *Adv. Mater.* **2001**, *13*, 95–108.
- (11) Lee, I.; Wool, R. P. *Macromolecules* **2000**, *33*, 2680–2687.
- (12) Lee, I.; Wool, R. P. *J. Polym. Sci., Polym. Phys. Ed.* **2002**, *2343*–2353.
- (13) Lee, I.; Wool, R. P. *J. Adhes.* **2001**, *75*, 299–323.
- (14) Lee, I.; Wool, R. P. *Thin Solid Films* **2000**, *379*, 94–100.
- (15) Barchini, R.; Gordon, J. G.; Hart, M. W. *Jpn. J. Appl. Phys. Part I—Regul. Pap. Short Notes Rev. Pap.* **1998**, *37*, 6662–6668.
- (16) Bowley, C. C.; Crawford, G. P. *Appl. Phys. Lett.* **2000**, *76*, 2235–2237.
- (17) Lee, J. W.; Pathangey, B.; Davidson, M. R.; Holloway, P. H.; Lambers, E. S.; Davydov, B.; Anderson, T. J.; Pearton, S. J. *J. Vac. Sci. Technol. A—Vac. Surf. Films* **1998**, *16*, 2177–2186.
- (18) Witten, T. A.; Sander, L. M. *Phys. Rev. Lett.* **1981**, *47*, 1400–1403.
- (19) Witten, T. A.; Sander, L. M. *Phys. Rev. B* **1983**, *27*, 5686–5697.

(20) Vicsek, T. *Fractal Growth Phenomena*; World Scientific: Singapore, 1989.

(21) Barabasi, A.-L. *Fractal Concepts in Surface Growth*; Cambridge University Press: Cambridge, 1995.

(22) Gmachowski, L. *Colloid Surf. A—Physicochem. Eng. Asp.* **2002**, *211*, 197–203.

(23) Jensen, M. H.; Mathiesen, J.; Procaccia, I. *Phys. Rev. E* **2003**, *67*, art. no.-042402.

(24) Lin, B.; Sureshkumar, R.; Kardos, J. L. *Chem. Eng. Sci.* **2003**, *58*, 2445–2447.

(25) Ouyang, W. Z.; Tan, Z. H.; Zou, X. W.; Jin, Z. Z. *Chaos Solutions Fractals* **2003**, *17*, 189–193.

(26) Xuan, Y. M.; Li, Q.; Hu, W. F. *AIChE J.* **2003**, *49*, 1038–1043.

(27) Ye, G. X.; Xia, A. G.; Gao, G. L.; Lao, Y. F.; Tao, X. M. *Phys. Rev. B* **2001**, *63*, 5405.

(28) Wang, S. Z.; Xin, H. W. *J. Phys. Chem. B* **2000**, *104*, 5681–5685.

(29) Berg, D. B. *Technol. Phys. Lett.* **1999**, *25*, 962–964.

(30) Gonzalez, A. E.; Lach-Hab, M.; Blaisten-Barojas, E. *J. Sol-Gel Sci. Technol.* **1999**, *15*, 119–127.

(31) Wen, W. J.; Zheng, D. W.; Tu, K. N. *Phys. Rev. E* **1998**, *58*, 7682–7685.

(32) Sheu, C. R.; Cheng, C. Y.; Pan, R. P. *Phys. Rev. E* **1999**, *59*, 1540–1544.

(33) Koneripalli, N.; Bates, F. S.; Fredrickson, G. H. *Phys. Rev. Lett.* **1998**, *81*, 1861.

(34) Langer, J. S. *Rev. Mod. Phys.* **1980**, *52*, 1–28.

(35) Honjo, H.; Ohta, S.; Matsushita, M. *J. Phys. Soc. Jpn.* **1986**, *55*, 2487–2490.

(36) Spengler, J. F.; Coakley, W. T. *Langmuir* **2003**, *19*, 3635–3642.

(37) Brady, R. M.; Ball, R. C. *Nature* **1984**, *309*, 225–229.

(38) Daccord, G.; Nittmann, J. *Phys. Rev. Lett.* **1986**, *56*, 336–339.

macroscopic aspects of structure formation governed by the universal nature of structural order.^{18,19,38-48}

Since the layer-by-layer (LBL) assembly technique was first introduced,⁴⁹⁻⁵⁴ much research has been done in the past decade to fabricate polymer and organic thin films via alternating adsorption of positively and negatively charged species on solid surfaces. Thin film processing by LBL techniques became one of the important thin film processes in electrooptic,⁵⁵⁻⁶¹ electroluminescent,⁶²⁻⁶⁵ conducting,⁶⁶⁻⁷⁰ and dielectric layers^{71,72} and with functional organic and inorganic nanoparticles.⁷³⁻⁸⁰ On the other hand, after the "soft lithography" technique was

successfully introduced, it has also been modified to fabricate more complex patterns on surfaces.⁸¹⁻⁸⁴ However, most soft lithographic processing, as required in "photolithographic" processing, needs pre- or postprocessing to complete the surface patterns.^{81,85,86} For example, alkane thiols or silanes were first patterned on gold or silicon oxide, glass, and metal oxides using microcontact printing (μ CP). Then polyelectrolytes or polymer precursors, metal ions or particles, colloids or chemically modified polymer latex particles, and biomaterials such as DNA, proteins, and cells are selectively deposited to complete the surface patterns.⁸⁷⁻⁹⁷ Soft lithography and LBL techniques have been combined to fabricate more complex 2-D and 3-D micron- and submicron-sized structures on surfaces.^{12,84,98-104} Such recent developments have made it simple and possible to create patterned functional surfaces, using the "polymer-on-polymer stamping (POPS) technique". In this work, a monolayer of polymer is transferred to a polymer substrate with complementary functional groups using microcontact printing. The formation of polymer aggregates was avoided through the optimization of the ink and stamping process.^{84,103,105,106} Using POPS techniques, it is possible to use plastics, glasses,

(39) Holzwarth, A.; Leporatti, S.; Riegler, H. *Europhys. Lett.* **2000**, *52*, 653-659.

(40) Tan, Z. J.; Zou, X. W.; Zhang, W. B.; Jin, Z. Z. *Phys. Lett. A* **2000**, *268*, 112-116.

(41) Tan, Z. J.; Zou, X. W.; Zhang, W. B.; Jin, Z. Z. *Phys. Rev. E* **1999**, *60*, 6202-6205.

(42) Ariga, K.; Lvov, Y.; Kunitake, T. *J. Am. Chem. Soc.* **1997**, *119*, 2224-2231.

(43) Halsey, T. C. *Phys. Today* **2000**, *53*, 36-41.

(44) Zheng, D. W.; Wen, W. J.; Tu, K. N. *Phys. Rev. E* **1998**, *57*, R3719-R3722.

(45) Hill, S. C.; Alexander, J. I. D. *Phys. Rev. E* **1997**, *56*, 4317-4327.

(46) Halsey, T. C.; Duplantier, B.; Honda, K. *Phys. Rev. Lett.* **1997**, *78*, 1719-1722.

(47) Vandewalle, N.; Ausloos, M. *Phys. Rev. E* **1995**, *51*, 597-603.

(48) Halsey, T. C. *Phys. Rev. Lett.* **1994**, *72*, 1228-1231.

(49) Decher, G. *Science* **1997**, *277*, 1232.

(50) Decher, G.; Hong, J. D. *Makromol. Chem.-Macromol. Symp.* **1991**, *46*, 321-327.

(51) Decher, G.; MacLennan, J.; Sohling, U.; Reibel, J. *Thin Solid Films* **1992**, *210*, 504-507.

(52) Lvov, Y.; Haas, H.; Decher, G.; Mohwald, H.; Mikhailov, A.; Mchedlishvili, B.; Morgunova, E.; Vainshtein, B. *Langmuir* **1994**, *10*, 4232-4236.

(53) Ruths, J.; Essler, F.; Decher, G.; Riegler, H. *Langmuir* **2000**, *16*, 8871-8878.

(54) Schmidt, R.; Decher, G.; Mesini, P. *Tetrahedron Lett.* **1999**, *40*, 1677-1680.

(55) Druy, M. A.; Rubner, M. F.; Sichel, E. K.; Tripathy, S. K.; Emma, T.; Cukor, P. *Mol. Cryst. Liq. Cryst.* **1984**, *105*, 109-122.

(56) Sichel, E. K.; Rubner, M. F. *J. Polym. Sci. Pt. B-Polym. Phys.* **1985**, *23*, 1629-1636.

(57) Kaneko, F.; Dresselhaus, M. S.; Rubner, M. F.; Shibata, M.; Kobayashi, S. *Thin Solid Films* **1988**, *160*, 327-332.

(58) Decher, G.; Tieke, B.; Bosshard, C.; Gunter, P. *J. Chem. Soc., Chem. Commun.* **1988**, 933-934.

(59) Watanabe, I.; Hong, K.; Rubner, M. F. *Thin Solid Films* **1989**, *179*, 199-206.

(60) Booth, B. L. In *Polymers for Electronic and Photonic Applications*; Wong, C. P., Ed.; Academic Press: Boston, 1993; pp 549-597.

(61) Sukhishvili, S. A.; Granick, S. *J. Chem. Phys.* **1998**, *109*, 6861-6868.

(62) Kim, Y.; Kwon, S.; Yoo, D.; Rubner, M. F.; Wrighton, M. S. *Chem. Mater.* **1997**, *9*, 2699.

(63) Kim, S.; Jackiw, J.; Robinson, E.; Schanze, K. S.; Reynolds, J. R.; Baur, J.; Rubner, M. F.; Boils, D. *Macromolecules* **1998**, *31*, 964-974.

(64) Lee, J. K.; Yoo, D. S.; Handy, E. S.; Rubner, M. F. *Appl. Phys. Lett.* **1996**, *69*, 1686-1688.

(65) Lee, J. K.; Yoo, D.; Rubner, M. F. *Chem. Mater.* **1997**, *9*, 1710.

(66) Chen, J. M.; Yang, X. Q.; Chapman, D.; Nelson, M.; Skotheim, T. A.; Ehrlich, S. N.; Rosner, R. B.; Rubner, M. F. *Mol. Cryst. Liq. Cryst.* **1990**, *190*, 145-153.

(67) Cheung, J. H.; Fou, A. F.; Rubner, M. F. *Thin Solid Films* **1994**, *244*, 985-989.

(68) Fou, A. C.; Onitsuka, O.; Ferreira, M. S.; Howie, D.; Rubner, M. F. In *ACS Meeting Proceedings, Spring Meeting, Anaheim, CA, 1995*.

(69) Royappa, A. T.; Rubner, M. F. *Langmuir* **1992**, *8*, 3168-3177.

(70) Wang, Y. D.; Rubner, M. F.; Buckley, L. J. *Synth. Met.* **1991**, *41*, 1103-1108.

(71) Durstock, M. F.; Rubner, M. F. *Langmuir* **2001**, submitted.

(72) Sichel, E. K.; Rubner, M. F.; Druy, M. A.; Gittleman, J. I.; Bozowski, S. *Phys. Rev. B* **1984**, *29*, 6716-6721.

(73) Aliev, F. G.; Correa-Duarte, M. A.; Mamedov, A.; Ostrander, J. W.; Giersig, M.; Liz-Marzan, L. M.; Kotov, N. A. *Adv. Mater.* **1999**, *11*, 1006-1010.

(74) Brust, M.; Etchenique, R.; Calvo, E. J.; Gordillo, G. J. *Chem. Commun.* **1996**, 1949-1950.

(75) Dante, S.; Hou, Z. Z.; Risbud, S.; Stroeve, P. *Langmuir* **1999**, *15*, 2176-2182.

(76) Kotov, N. A.; Mamedov, A. A.; Koktysh, D.; Mussig, S.; Ostrander, J. *Abstr. Pap. Am. Chem. Soc.* **2000**, *219*, 382-COLL.

(77) Lvov, Y.; Ariga, K.; Onda, M.; Ichinose, I.; Kunitake, T. *Langmuir* **1997**, *13*, 6195.

(78) Ostrander, J. W.; Mamedov, A. A.; Kotov, N. A. *J. Am. Chem. Soc.* **2001**, *123*, 1101-1110.

(79) Schmitt, J.; Decher, G.; Dressick, W. J.; Brandow, S. L.; Geer, R. E.; Shashidhar, R.; Calvert, J. M. *Adv. Mater.* **1997**, *9*, 61.

(80) Schrof, W.; Rozouvan, S.; Van Keuren, E.; Horn, D.; Schmitt, J.; Decher, G. *Adv. Mater.* **1998**, *10*, 338-341.

(81) Qin, D.; Xia, Y. N.; Rogers, J. A.; Jackman, R. J.; Zhao, X. M.; Whitesides, G. M. *Microsystem Technol. Chem. Life Sci.* **1998**, *194*, 1-20.

(82) Xia, Y. N.; Whitesides, G. M. *Angew. Chem. Int. Ed. Engl.* **1998**, *37*, 551-575.

(83) Yin, Y. D.; Gates, B.; Xia, Y. N. *Adv. Mater.* **2000**, *12*, 1426-1430.

(84) Jiang, X.-P. H.; P. T. *Langmuir* **2000**, *16*, 8501-8509.

(85) Prucker, O.; Schimmel, M.; Tovar, G.; Knoll, W.; Rühle, J. *Adv. Mater.* **1998**, *10*, 1073-1077.

(86) Xia, Y. N.; Zhao, X. M.; Whitesides, G. M. *Microelectron. Eng.* **1996**, *32*, 255-268.

(87) Decher, G.; Ringsdorf, H. *Liq. Cryst.* **1993**, *13*, 57-69.

(88) Decher, G.; Lehr, B.; Lowack, K.; Lvov, Y.; Schmitt, J. *Biosens. Bioelectron.* **1994**, *9*, 677-684.

(89) Ladam, G.; Gergely, C.; Senger, B.; Decher, G.; Voegel, J. C.; Schaaf, P.; Cuisinier, F. J. G. *Biomacromolecules* **2000**, *1*, 674-687.

(90) Ladam, G.; Schaaf, P.; Cuisinier, F. J. G.; Decher, G.; Voegel, J. C. *Langmuir* **2001**, *17*, 878-882.

(91) Caruso, F.; Mohwald, H. *J. Am. Chem. Soc.* **1999**, *121*, 6039-6046.

(92) Jeon, S. I.; Lee, J. H.; Andrade, J. D. *J. Colloid Interface Sci.* **1991**, *142*, 149-158.

(93) Jeon, S. I.; Andrade, J. D. *J. Colloid Interface Sci.* **1991**, *142*, 159-166.

(94) Lee, J. H.; Kopecek, J.; Andrade, J. D. *J. Biomed. Mater. Res.* **1989**, *23*, 351-368.

(95) Mrksich, M.; Dike, L. E.; Tien, J.; Ingber, D. E.; Whitesides, G. M. *Exp. Cell Res.* **1997**, *235*, 305-313.

(96) Prime, K. L.; Whitesides, G. M. *J. Am. Chem. Soc.* **1993**, *115*, 10714-10721.

(97) Lvov, Y.; Decher, G.; Sukhorukov, G. *Macromolecules* **1993**, *26*, 5396-5399.

(98) Clark, S. L.; Montague, M.; Hammond, P. T. *Supramol. Sci.* **1997**, *4*, 141-146.

(99) Clark, S. L.; Montague, M. F.; Hammond, P. T. *Macromolecules* **1997**, *30*, 7237-7244.

(100) Clark, S. L.; Hammond, P. T. *Adv. Mater.* **1998**, *10*, 1515.

(101) Clark, S. L.; Handy, E. S.; Rubner, M. F.; Hammond, P. T. *Adv. Mater.* **1999**, *11*, 1031-1035.

(102) Clark, S. L.; Hammond, P. T. *Langmuir* **2000**, *16*, 10206-10214.

(103) Jiang, X. P. Z.; H.; Gourdin, S.; Hammond, P. T. *Adv. Mater.* **2001**, submitted.

(104) Zheng, H.; Lee, I.; Rubner, M. F.; Hammond, P. T. *Adv. Mater.* **2002**, *14*, 569-572.

(105) Jiang, X. P. C.; B.; Choi, J.; Rubner, M. F.; Hammond, P. T. Manuscript in preparation.

(106) Jiang, X.; Zheng, H.; Gourdin, S.; Hammond, P. T. *Langmuir* **2002**, *18*, 2607-2615.

and other substrates without the use of gold, thus making the POPS approach cheap and applicable to a new range of materials.¹⁰⁶ Polymer stamping has a great deal of potential to fabricate patterned functional layers on surfaces on micron or submicron scale using a single-step process, which removes many unnecessary steps that are normally used in the photolithographic approach to surface patterning.

In this paper, we demonstrate for the first time how to control the two-dimensional polyelectrolyte aggregates created by microcontact printing. A key feature of this work is the thin film morphology study of microcontact printed polyelectrolyte aggregates. The polyelectrolyte ink and stamping processes were designed for the formation of polyelectrolyte aggregates (e.g., tree-like ramified structures). We report the coarsening of the ramified structures of polyelectrolyte by confining the stamp's contact area to a size in which the pattern is smaller than that of the ramified structures. In addition, we report that the ramified structures can be directed by directional stamping without conformal contact at the interface. The controlled polyelectrolyte aggregates were investigated after extensive washing with deionized (DI) water, by selective electroless nickel plating and charged particle depositions.

Experimental Section

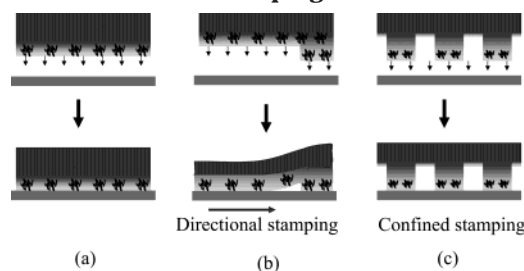
Microcontact Printing of Polyelectrolyte Aggregations.

Polydimethylsiloxane (PDMS, Dow Corning) stamps were prepared using a Cr photo mask (Advanced Reproduction, Andover, MA) and corresponding silicon master (Microsystems Technology Lab, MIT). Both the PDMS stamps and glass slides were treated with oxygen plasma for 15 s (stamp) and for 1–5 min (glass slide) at a pressure of 0.2 Torr using a Harrick plasma cleaner to create surface oxidation, which causes the hydrophobic PDMS stamp surface to become hydrophilic. Two different substrates were used: oxygen plasma treated glass surfaces and negatively charged polyelectrolyte multilayers. Leaving the topmost surface negatively charged, 10 bilayers of charged polyelectrolyte multilayers were deposited on the glass slides using a standard procedure described elsewhere.¹⁰⁷ Sulfonated polystyrene (SPS, Aldrich, $M_w = 70\,000$) was used as the polyanion and poly(dimethylallylammonium chloride) (PDAC, Aldrich, $M_w = 150\,000$) was used as the polycation. The PDAC polymer ink solution (10 mM PDAC and 0.05 M NaCl in 50/50 vol % ethanol/water) used to transfer the polymer onto the oxygen plasma treated glass surface was slightly different than the PDAC ink solution (20 mM PDAC and 0.1 M NaCl in 100% water) used to transfer polymer onto the negatively charged SPS surface.

The hydrophilic PDMS stamp surfaces are inked with PDAC using cotton-tipped applicators once or multiple times to change the amount of ink on the surface of the stamp. The stamps were then dried under air for 5 min. Air or nitrogen was not blown on the surface. Then, the stamps were put on top of a glass slide without any force for 1 min to 30 min. Good contact of the inked PDMS stamp on the glass slide surface was automatically made by wetting forces and confirmed by the naked eye. After removing the PDMS stamps from the glass slide, the polymer pattern transferred to the glass slide was examined using a Nikon Eclipse ME 600 microscope. After the micropatterned PDAC aggregates were completely washed away with DI water, the resulting substrates were further investigated using a selective nickel plating technique¹⁰⁸ and negatively charged colloidal particle deposition to identify the patterned region on the glass slides.¹⁰⁷

Controlling Fractal Growth and Aggregations. Scheme 1 illustrates three methods of polymer stamping used to control the fractal aggregations in this work. Depending on surface functional groups, the polyelectrolyte ink is expected to have specific interactions with the surface receptor groups by hydrogen

Scheme 1. Schematic Illustrations of Controlling Polyelectrolyte Fractal Growth and Aggregations created by μ CP: (a) Homogeneous (No Pattern) Stamping, (b) Directional Stamping, and (c) Confined Stamping



bonding, electrostatic interaction, or covalent bonding. The interactions between the polyelectrolyte sticker groups and surface receptor groups at interfaces are one of the main controlling factors^{11,13,14} in polymer stamping. Polymer ink is supposed to be easily soaked into the hydrophilic oxygen plasma treated PDMS surface layers. After the inked PDMS stamps are put on glass surfaces, the surface layer PDAC molecules start to restructure or diffuse out of the PDMS surface layers onto the glass surfaces. The first polymeric layer formed on the solid surfaces should be significant enough to transfer the polymer films from the stamp to the surfaces. The weakly adsorbed aggregates, which are characterized by an optical microscope, are intensively washed and leave optically transparent films that are possibly monolayer-like films. Identification of the ionically adsorbed first transparent layer is possible by depositing nickel on the chemically patterned transparent films by selective electroless deposition.¹⁰⁷ This selective electroless deposition of nickel can confirm the existence of the two different layers. Furthermore, the extra polymer chain diffusion toward the adsorbed primary layers, showing the fractal growth and aggregation processes, is determined by the competition between diffusion-limited transport and interfacial tension.^{18–21,33,35,37–41,43–48,109,110} Scheme 1a–c illustrates the three types of stamping methods performed to investigate the 2-D aggregation growth of stamped polymer layers on surfaces, where part a represents the case when pattern size is much bigger than that of the fractal domain on surfaces (i.e., homogeneous stamping). Part b covers the case of nonconformal contact between the stamp and surfaces, directing the fractal growth and aggregation (i.e., directional stamping), and part c describes the case when the pattern size is smaller than the fractal domain (i.e., confined stamping). Using these various stamping types, the thin film morphology of ramified structures transferred on surfaces can be controlled.

Nickel Staining. Before selective nickel plating, the PDAC-micropatterned glass slides created by μ CP were washed extensively with DI water for 20 s. This was repeated three times in pure DI water to remove all the physically adsorbed secondary PDAC aggregate layers until the micropatterned glass slide became completely transparent in the entire stamped region. The washed samples were dipped into the catalytic solution, an aqueous Na_2PdCl_4 (Strem, Newburyport, MA) solution (1 mM), for 10 s, and then washed extensively with DI water for 2 min, and finally dipped into a nickel bath at room temperature for 10 min.¹⁰⁸ The electroless nickel bath contains nickel sulfate (Ni source, 4 g; Aldrich), sodium citrate (complexant, 2 g; Alfa Aesar, Ward Hill, MA), lactic acid (buffer, complexant, 1 g; Alfa Aesar), and dimethylamine borane (reductant, 0.2 g; Acros Organics, Fair Lawn, NJ) in 100 mL of DI water.¹¹¹ The pH of the Ni bath was adjusted to be 6.5 ± 0.2 using ammonium hydroxide (Aldrich).

Depositing Charged Particles. Sulfated polystyrene latex particles (negatively charged; surfactant-free; hydrophobic; $D = 0.5\ \mu\text{m}$, Interfacial Dynamics) were deposited onto the micro-

(109) Conti, M.; Meerson, B.; Satorov, P. V. *Phys. Rev. Lett.* **1998**, *80*, 4693–4696.

(110) Arneodo, A.; Argoul, F.; Couder, Y.; Rabaud, M. *Phys. Rev. Lett.* **1991**, *66*, 2332–2335.

(111) Wang, T. C.; Chen, B.; Rubner, M. F.; Cohen, R. E. *Langmuir* **2001**, *17*, 6610–6615.

(107) Lee, I.; Zheng, H.; Rubner, M. F.; Hammond, P. T. *Adv. Mater.* **2002**, *14*, 572–577.

(108) Lee, I.; Hammond, P. T.; Rubner, M. F. *Chem. Mater.* **2003**, *15*, 4583–4589.

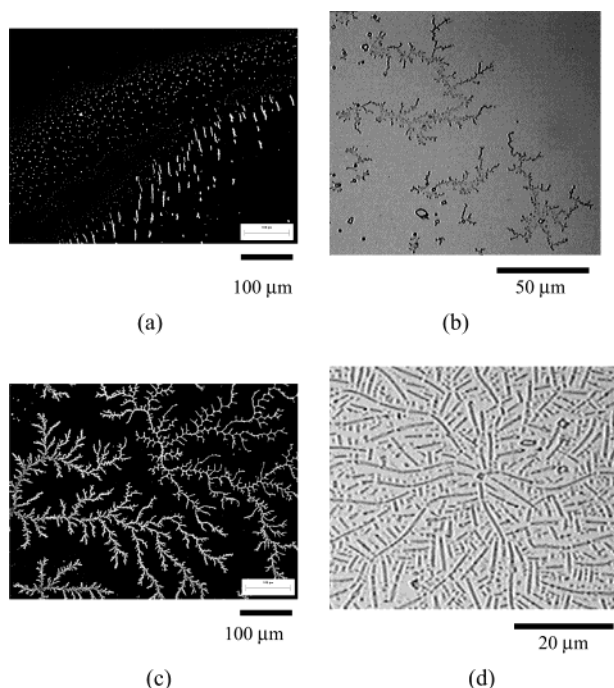


Figure 1. Optical micrographs of polycation (PDAC) fractal growth and aggregations created by μ CP on either SPS surfaces for 30 min or glass slides for 15 min. (a) A dark-field image of many starting aggregation points on a SPS surface. (b) A bright-field image of underdeveloped ramified structures on a glass surface. (c) A dark-field image of PDAC ramified structures on a SPS surface. (d) A bright field image of overdeveloped ramified structures on a glass surface.

patterned polycationic region in an aqueous solution.¹⁰⁷ As was done in the nickel plating, the PDAC-micropatterned glass slides created by μ CP were washed exclusively with DI water before charged particle deposition. This washing removes all the physically adsorbed PDAC aggregates off the patterned glass slide. The washed transparent samples were put upside down in the colloidal aqueous solution of 0.5 wt % without any surfactant or salt. After colloidal deposition, the samples were washed with DI water for 10 s.

Results and Discussion

Polyelectrolyte Fractal Growth and Aggregations by Microcontact Printing. Figure 1 shows the various optical micrographs of PDAC aggregates formed on surfaces by the μ CP technique. All the polyelectrolyte aggregates on the surfaces were amorphous aggregated films as confirmed by polarized optical micrographs. Parts a–d show the different stages of development for typical 2-D polyelectrolyte ramified structures, by a homogeneous PDMS stamp (see Scheme 1a). Using the same contact time and controlling the amount of ink on the stamp led to the observed progression of 2-D aggregates (a–d). The domain size was up to several hundred micrometers for well-developed 2-D ramified aggregates (see part c). Such treelike ramified structures are known as “diffusion-limited aggregations”,^{23–25,112} or “reaction limited aggregations”,^{36,113–115} In this work, it was not clear whether the aggregation formed purely by diffusion-limited aggregation or by reaction-limited aggregation. This is because

the PDAC ramified structures look more like the diffusion-limited aggregation type, but the interactions between the inked molecules and surface functional groups also played an important role in aggregation formation. However, it is believed that both the surface reaction and the surface layer diffusion or restructuring affected the formation of the ramified structures. The domain size of underdeveloped structures is on the order of 1 μ m (see Figure 1a) to 50 μ m (see Figure 1b). The typical ramified structures, also known as diffusion-limited aggregations, are widely observed in many different systems, such as fractal growth in strained block copolymer films,³³ molecular ordering and domain morphology of molecularly thin triacontane films,³⁹ antimony islands grown on graphite surfaces,¹¹⁶ and even computer simulated results by a nonequilibrium aggregation model such as diffusion-limited aggregation.^{19–21,23,37,40,41,43,109,112} It is known that the development of ramified structures, or fractal morphology, is governed by a competition between either reaction-limited phenomena or diffusion-limited transport and interfacial tension,³³ where any heterogeneous points act as a nucleating point of the following structures. On the other hand, when lots of polymer ink was applied on the same stamp by repeated application of the ink, such aggregations could be further developed due to excessive polyelectrolyte ink from the PDMS stamp. Many different fractal fronts from multiple origins meet to form connecting aggregates of growing ramified structures, as shown in Figure 1d. In general, the dynamics of the diffusion-controlled system follows these four steps: an unstable growth, coarsening, fragmentation, and an approach to equilibrium.¹⁰⁹ From Figure 1a–d, the order of such aggregation steps could be in the order of a, b, c, and d. But in the case of a, due to the many nucleating points of the aggregates, it is not likely to form fully developed ramified structures such as c, but relatively uniform films with less aggregation. However, some of the nucleating points in type a could dominate the further development of fractal growth to be like type c aggregates. It is noted that the various types of film formations are dependent on many different conditions such as surface roughness and energetics, ink and salt concentrations, and solvent.

Controlled Fractal Growth and Aggregations.

Figure 2 shows the control of the 2-D polyelectrolyte aggregates as described in Scheme 1: When directional polymer stamping was performed (see Scheme 1b), the fractal front of the ramified structure grows in the same direction as polymer stamping. Regardless of normal microcontact process with a conformal contact of a 90° angle, the directional stamping has a larger contact angle between the elastomeric stamp and the surface (>90°). This caused directional growth of the ramified structures, as shown in Figure 2a. In addition, polymer stamping on a confined surface area (see Scheme 1c) which is smaller than the domain size of the general ramified PDAC structures caused the fractal growth of the ramified structures to stay in a domain within the small contacted area of the stamp, as observed in Figure 2a,b. Inside the areas where the PDMS stamp contacted glass, the PDAC ink that was adsorbed into the stamp surface layers diffused from the stamp out onto the glass surface.

The confined PDAC ramified aggregates in parts a (right side) and b of Figure 2 show fragmented fractal growth structures and the conflicts among the isolated fractal

(112) Balgar, T.; Bautista, R.; Hartmann, N.; Hasselbrink, E. *Surf. Sci.* **2003**, *532*, 963–969.

(113) Behrens, S. H.; Christl, D. I.; Emmerzael, R.; Schurtenberger, P.; Borkovec, M. *Langmuir* **2000**, *16*, 2566–2575.

(114) Chatellier, X.; Bottero, J. Y.; Le Petit, J. *Langmuir* **2001**, *17*, 2791–2800.

(115) Tirado-Miranda, M.; Schmitt, A.; Callejas-Fernandez, J.; Fernandez-Barbero, A. *Langmuir* **1999**, *15*, 3437–3444.

(116) Yoon, B.; Akulin, V. M.; Cahuzac, P.; Carlier, F.; de Frutos, M.; Masson, A.; Mory, C.; Colliex, C.; Brechignac, C. *Surf. Sci.* **1999**, *443*, 76–88.

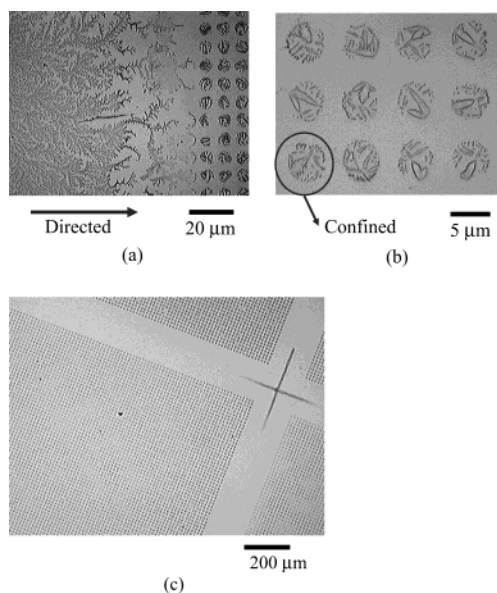


Figure 2. Optical micrographs of polycation (PDAC) fractal growth and aggregations on glass slides controlled by μ CP. (a) A dark-field image of directed (to the right) fractal growth by directed polymer stamping, (b) isolated fractal growth of polymer thin film aggregation, and (c) polymer micropatterning over a large area (b and c are in bright-field mode).

structures after the unstable growth and coarsening (thickening process of the fractal branch) steps. The two patterns (left-directional growth, right-confined growth) in Figure 2a,b look different. The confined fractal growth of the polyelectrolyte aggregations in the confined area reaches the fragmentation stage faster than the directed fractal growth. The fractal tips of the aggregations confined within a contact area grow until they reach the edge where they are bounced back internally and continue to grow within the contacted area. This might support the theory of Conti et al.,¹⁰⁹ which suggests that the diffusion-controlled phase ordering of fractal clusters is not a scale-invariant process and that an additional length scale of the coarsening process remains relevant until the fragmentation stage.

Restructuring of PDAC-Inked Surface Layers and 2-D Aggregations. The PDAC-ramified aggregations showed a strong dependence on contact time, as well as the amount of ink present on the stamp. When using glass surfaces, contact times less than 10 min did not follow the aggregation process observed in Figure 1. Contact times from 15 min up to 30 min did not have a major difference in the confined film morphology. In this work, the saturation contact times were found to be around 10–15 min, regardless of the amount of ink. The wetting properties of the PDMS stamp are very important in inking the stamp. The oxygen plasma treatment of the stamp allowed the polymer solution to wet the PDMS surface. The surface layers of the PDMS stamp made hydrophilic by a brief plasma treatment can restructure to dewet the wetted polymer inks for the purpose of transferring. This restructuring process of the PDMS surface layers was qualitatively confirmed by contact angle measurements of the stamp. The advancing water contact angle changed considerably with time. Initially it was $110^\circ \pm 4^\circ$, and then it reduced to $27^\circ \pm 5^\circ$ immediately after a 15 s oxygen plasma treatment, and then it was around $80^\circ \pm 8^\circ$ after exposure to air for 24 h. This may indicate the restructuring of the PDMS stamp surface layers, which helps the polyelectrolyte ink diffuse out of the stamp to the glass surface. While using the oxygen plasma treated PDMS

stamp with polymer ink repeatedly, it was found that the wetting properties of stamp surface changed very quickly after a couple of hours. Initially, just after the O_2 plasma treatment, lots of silanol groups ($-SiOH$) are generated on the outer surface (confirmed by the reduced water contact angle); however, due to the enthalpic and entropic instability, the modified PDMS surface layers restructure themselves. The highly energetic silanol groups on the outer surface are hiding beneath the top surface layers or are contaminated with impurities that exist in air, such as carbon dioxide, bicarbonate, and other dusts, which are responsible for the time-dependent change in contact angle. The restructuring process of the polymer surface layers that are dependent on the enthalpic and entropic constraints of the interface is a well-known phenomena.^{11–13,117} Using this phenomenon, polymer stamping on solid surfaces such as glass, silicon oxide, and metal oxide can be pursued. With the help of a solvent, polymers can easily be placed inside the surface layers of a plasma-treated PDMS stamp. After placing the stamp on top of a plasma-treated glass slide, very thin polymer films are generated by the diffusive transport of polymers from the stamp surface layers onto the glass surfaces. The outer functional groups of the glass are also the same silanol groups ($-SiOH$) as on the oxygen plasma treated stamp. At the glass–stamp interface, the PDAC from either diffusion out of the stamp or hanging on the stamp surfaces can strongly adsorb through the electrostatic interactions of the polymer sticker groups and the substrate receptor groups on the glass surface.^{11–13} This process depends on the amount of solvent vapor and an appropriate contact time. However, the polymer attachment to the stamp surface weakens as the restructuring process goes on. Finally, the polymer film is more strongly bound on the glass surface, where the silanol groups of the glass surface are more stable than those of the PDMS stamp surface. Polymer stamping is unlike the layer-by-layer assembly of dilute strong polyelectrolyte solutions in which the second polymer layer is easily repelled by the adsorbed polymer layer by electrostatic repulsion, which forms uniform monolayers. Instead polymer stamping basically deposits multilayers onto solid surfaces where the first layer can be strongly adsorbed due to specific interactions such as hydrogen bonding, electrostatic interaction, and covalent bonding between the solid surface and the polymers. However with a further drying step, the second polymer layers are supposed to stand on the first layers by a kinetic effect in polymer stamping. The extra layers on top of the first strongly adsorbed layers seemed to cause irregular patterns on surfaces. This is because the first adsorbed layers are believed to be strongly adsorbed by the electrostatic interactions between the sticker groups of PDAC [$-N^+(CH_2)_2(CH_3)_3$] and the receptor groups of glass ($-SiOH^-$), but the additional layers above the first adsorbed layer cannot strongly bind on the first layer, thus forming weakly physisorbed layers that are responsible for the irregular patterns or aggregates on the surfaces that are visible with a microscope.

Primary and Secondary Layers of Polyelectrolyte Fractal Growth and Aggregations. The PDAC aggregates were further investigated. The existence of two different layers are identified by extensively washing the samples (removing the weakly adsorbed layers) and then by identifying the strongly adsorbed first layers on glass with selective nickel plating (see Figure 3) and colloidal deposition techniques (see Figure 4).

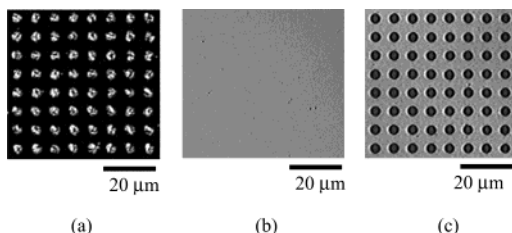


Figure 3. Optical micrographs of nickel staining polycation (PDAC) stamped micropatterns on glass slides: (a) dark-field image, (b) after a careful washing with DI water (transparent), and (c) nickel stained micropatterns on glass for 10 min after a washing step.

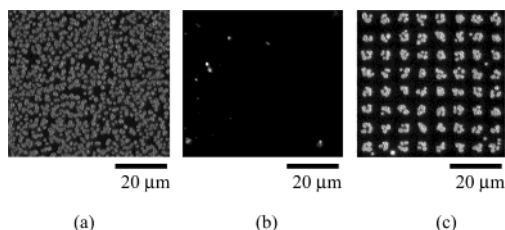


Figure 4. Optical micrographs (dark-field mode) of ionic colloidal deposition on polycationic micropatterns: (a) on the homogeneous polymer (blank) stamped, (b) on unstamped region, and (c) on micropatterned polycationic region on glass. Before the colloidal deposition, the samples were carefully washed with DI water to remove all the physisorbed secondary layers.

Figure 3 shows optical micrographs of polyelectrolyte aggregate micropatterns on oxygen plasma treated glass (a) unwashed (diffusion-limited aggregation on confined area in dark-field mode), (b) after washing (became transparent by removing the physisorbed aggregates) with DI water, and (c) nickel plated on the transparent sample shown in panel b. The polarized optical micrographic analysis indicated that the ramified polymer structures are just aggregated solid, not crystallized structures. The important observation of the selective nickel plating of the micropatterned transparent glass slides is that the first adsorbed monolayer-like PDAC micropattern on the bare glass slide cannot be washed away with DI water, while the secondary aggregate layers on the first adsorbed layer were easily washed away. This means that the first PDAC layer on glass forms a strongly adsorbed micropatterned polyelectrolyte layer on glass, and then additional polyelectrolyte molecules form the typical ramified pattern structures as seen in Figures 1 and 2. After washing the sample shown in Figure 3a with DI water for 5 min, the micropatterned samples showed no specific visible patterns (i.e., transparent) on the glass slides, as observed in Figure 3b. However, as the transparent micropatterned sample shown in Figure 3b was stained in the nickel bath by the selective electroless deposition, the transparent PDAC micropatterns on glass can clearly be seen again (see Figure 3c). This is because of the differential nickel depositions on the micropatterned samples. In the selective nickel plating process, the washed samples were first treated with a Pd complex, $[\text{PdCl}_4]^{2-}$, that preferentially binds on the PDAC patterned area (inside of the circles), and then in the nickel bath nickel ions were preferentially reduced inside the circular area. After 10 min, the transparent sample (see Figure 3b) changed to look like the sample of Figure 3c due to the differential nickel plating. In this work, a selective nickel plating technique was used to identify the first adsorbed layers that were shown as uniform and transparent micropatterns, not the same fractal-like films with the additional layers. In a forthcoming paper, we will dem-

onstrate the selective nickel deposition on the micropatterned glass with another Pd catalyst complex.

As shown in Figure 4, the transparent PDAC micropatterns on glass (samples washed as shown in Figure 3b) were further confirmed by negatively charged particle deposition. Negatively charged sulfated polystyrene latex particles ($D = 0.5 \mu\text{m}$) were deposited onto the positively charged PDAC-micropatterned surface in 0.5 wt % aqueous solution, in which the patterned surface was put upside down in the colloidal solution for 3 min to remove the effect of gravity. Due to the electrostatic interactions in water solution between the negatively charged colloid and the positively charged PDAC areas, 2-D colloidal patterns on glass slides were fabricated, as shown in Figure 4c; parts a, b, and c (homogeneous PDAC layer, unprinted area, and circle-patterned PDAC arrays on glass, respectively) of Figure 4 taken from the same sample surfaces show the clear PDAC pattern on glass slides. Regular patterned colloidal arrays (see Figure 4c) show brighter and clearer than the irregularly deposited colloid samples (see Figure 4a) when viewed on a microscope in dark field optical image mode. As shown in Figure 4c, the aggregation of charged particles on a surface is also related to the fractal growth and aggregation phenomena.

Conclusions

We demonstrated, for the first time, the formation and the control of the polyelectrolyte aggregations by μCP . The controlled polyelectrolyte aggregations (e.g., ramified structures) on surfaces formed two distinct layers. The primary layer was strongly bound on the glass surfaces by electrostatic interactions and was not washed away after extensive washing with DI water, unlike the secondary aggregated layer. The primary layer was identified by a selective nickel plating technique and charged particle deposition after removing the secondary aggregate layers by extensive washing. The primary layers of confined (e.g., micropatterned) polyelectrolyte aggregates created by μCP were uniform within the confined contacted areas after being fully developed (e.g., after coarsening and fragmentation steps in aggregation growth). The micropatterned primary layers of polycations were used to selectively deposit nickel and negatively charged colloidal particles. It was found that the secondary layers within a confined area formed the typical ramified structures (coarsened and fragmented within the 2-D confined microcontacted area) of the fractal growth and aggregation by phase ordering. The directional and confined stampings enabled us to control the polyelectrolyte fractal clusters. The polyelectrolyte fractal clusters created by μCP were easily removed by extensive washing with DI water, finally leaving the strongly adsorbed, monolayer-like polyelectrolyte micropatterns on surfaces, which can be important for devices and sensor applications.

Acknowledgment. The authors would like to thank Prof. You-Yeon Won at Purdue University for the discussion on the interfacial instabilities and fractal growth phenomena, and also to Dr. Tom C. Wang at MIT and Dr. Xueping Jiang at DuPont for the selective nickel-plating work. This work was funded by the Center for Fundamental Materials Research at the Michigan State University, Hitachi Chemical, Co., Ltd. and the Microphotonics Research Center and the Center for Materials Science and Engineering at the Massachusetts Institute of Technology.